Volume 8 | Number 19 | 21 May 2017 | Pages 2891–3036

Polymer Chemistry

rsc.li/polymers

ISSN 1759-9962

ROYAL SOCIETY OF CHEMISTRY

PAPER

Hongbing Deng *et al.*

Highly cost-effective and high-strength hydrogels as dye adsorbents from natural polymers: chitosan and cellulose

Polymer Chemistry

PAPER

View Article Online
View Journal | View Issue

Cite this: *Polym. Chem.*, 2017, **8**, 2913

Highly cost-effective and high-strength hydrogels as dye adsorbents from natural polymers: chitosan and cellulose

Hu Tu,†[a] Yi Yu,†[a] Jiajia Chen,[a] Xiaowen Shi,[a] Jialin Zhou,[a,b] Hongbing Deng *[a] and Yumin Du[a]

Received 9th February 2017,
Accepted 3rd March 2017

DOI: 10.1039/c7py00223h

rsc.li/polymers

Search for cost-effective and high-strength dye adsorbents has become an urgent problem in wastewater treatment. Natural polymers such as chitosan and cellulose are low-cost and can be fabricated as hydrogels for dye adsorption, but these hydrogels usually have weak strength. Here, novel high-strength and highly cost-effective hydrogels with a high capacity of dye adsorption were prepared with chitosan and cellulose. The chitosan/cellulose hydrogels could be knotted and twisted without fracture and could be restore rapidly after compression. These features showed that the hydrogels had good elasticity, high strength and excellent resilience. Also, the incorporation of rectorite into hydrogels could increase the thermal stability and strength of composite hydrogels. Subsequently, the adsorption capacity of hydrogels to Congo Red was investigated: chitosan was the main functional material for adsorption and rectorite participated in dye adsorption as well, but cellulose supported the structure. Furthermore, the adsorption process fitted closely with the Freundlich model, and was best described by a pseudo-second-order kinetic model. The hydrogels were biodegradable and could be easily collected after adsorption. These environmental friendly hydrogels could be promising candidates for dye removal in the future.

1. Introduction

Discharged wastewater containing dye compounds can create severe water-pollution problems in the industries of paper-making, printing, and textile dyeing.[1] Dye pollution can disturb the aquatic biosphere; dye compounds can bioaccumulate along food chains and, eventually, cause chronic toxicity to humans.[2] Natural polymers are used as ideal dye adsorbents because of their easy access, low cost, and efficient adsorption.[3] Natural polymers can be fabricated to different shapes for dye adsorption, such as membranes, microspheres and hydrogels.[4,5] However, these materials are usually short of mechanical performance, and the synthetic process is complicated. It is extremely difficult for materials to simultaneously have high mechanical performance, efficient dye adsorption and to be highly cost-effective and convenient to use in practical applications.[6] Therefore, finding efficient methods and cheap materials for fabricating adsorbents with outstanding mechanical performance is important.

Polysaccharides-based adsorbents have been widely studied owing to their high adsorption capacity, biodegradability and biocompatibility.[7,8] Chitin and cellulose based on living creatures have been used for solving environmental problems due to their easy availability, low cost and nontoxic nature.[9–11] Chitosan is the *N*-deacetylated product of chitin, which is the major component of shells of arthropods and crustaceans.[12,13] Chitosan as a cheap and available material has been widely used in bacterial inhibition, adsorption of metals and dyes, and tissue engineering.[3,14–16] It has been reported that chitosan has good sorption capacity for dye owing to the abundant amino acids acting as chelating sites.[3] However, the weak mechanical strength of chitosan-based materials limits their application as effective adsorbents. Cellulose is the most readily available and naturally renewable polysaccharide with unique physical and mechanical properties.[17] It also has hydroxyl groups that can combine dye molecules.[18] Thus, chitosan and cellulose can be combined to create novel composite hydrogels. These composite hydrogels are expected to boost the excellent properties of chitosan and cellulose to obtain unprecedented mechanical properties and efficient dye adsorption.

[a]*Hubei International Scientific and Technological Cooperation Base of Sustainable Resource and Energy, Hubei Key Laboratory of Biomass Resource Chemistry and Environmental Biotechnology, School of Resource and Environmental Science, Wuhan University, Wuhan 430079, China. E-mail: hbdeng@whu.edu.cn, alphabeita@yahoo.com; Fax: +86 27 68778501; Tel: +86 27 68778501*
[b]*College of Chemistry and Molecular Sciences, Wuhan University, Wuhan, 430072, China*
† Co-first authors who made equal contributions to this work.

Rectorite (REC) is a layered silicate. It has alternating dioctahedral mica-like and montmorillonite-like layers.[19] It has been reported that REC possesses several functional groups that can bind metal ions and charged dyes through coordination, electrostatic interaction and cation exchange.[20,21] Hence, we plan to explore the effect on the adsorption capability of hydrogels by introducing REC.

In the present study, the chitosan/REC/cellulose composite hydrogels with high strength were fabricated from biomass. These hydrogels were characterized to analyze their morphology, structure and thermostability. Compressive tests of the composite hydrogels were used to study their mechanical properties. Subsequently, the removal of Congo Red from aqueous solution under different adsorption parameters, such as initial concentrations, contact times as well as the compositions of adsorbents, was investigated to find out the adsorption behavior and performance of these novel hydrogels. The adsorption isotherms and kinetics were also investigated.

2. Experimental sections

2.1 Materials

Chitosan with a deacetylation degree >90% was purchased from Ruji Biological Science (China). Cellulose was provided by Hubei Jinhuan (China). REC was purchased from Hubei Mingliu Science (China). Epichlorohydrin (ECH) and other reagents of analytical grade were from Sinopharm Chemical Reagents (China).

2.2 Preparation of compound hydrogels

Briefly, 5% or 10% (wt/wt%) REC was dispersed under alkali/urea conditions *via* ultrasound equipment. Chitosan and cellulose were dissolved in several alkali/urea solutions *via* freezing–thawing to obtain 4.0 wt% transparent solution. Then, chitosan and cellulose solutions were mixed with composition ratios of 9 : 1, 3 : 1, 1 : 1, 1 : 3 and 1 : 9, respectively. REC suspensions and ECH were injected dropwise into the stirred chitosan/cellulose solutions. The whole mixtures were stirred by vigorous agitation for 2 h at −12 °C. Then, the composite solutions were centrifuged for 10 min at 5 °C and, finally, the sediments were slowly poured into the mold. The composite hydrogels were washed with deionized water and then freeze-dried by a lyophilizer (FreeeZone; Labconco, USA) for further testing.

2.3 Characterization

Field-emission scanning electron microscopy (FE-SEM) using a ∑IGMA instrument (Zeiss, Germany) was used to observe the morphology of composite hydrogels. The elementary composition analysis of the as-prepared samples was performed by Fourier-transform infrared (FT-IR) spectroscopy (170-SX; Thermo Nicolet, USA), energy-dispersive X-ray spectroscopy (EDS; GENESIS XM2; Gatan, USA) and X-ray photoelectron spectroscopy (XPS; Kratos, UK). Thermogravimetric analysis (TGA; SDT Q600; Tainstsh, USA) was carried out to investigate the thermal properties of the samples. X-ray diffraction (XRD) was characterized using a type D/max-Ra diffractometer (Rigaku, Japan). Compressive and stretching measurements were conducted using a tensile-compressive tester (CMT 6503; MTS/SANS, China).

2.4 The swelling behavior of hydrogels

The weighted composite hydrogels were put into different pH solutions for 3 days to ensure equilibrium swelling. Then, the wet mass of the hydrogels was determined again. The swelling ratio (SR) of the hydrogels could be calculated using the following formula:

$$\mathrm{SR}(\%) = \frac{W_\mathrm{w} - W_\mathrm{d}}{W_\mathrm{d}} \times 100\% \quad (1)$$

where W_w and W_d are the weight of the hydrogels before and after drying at 60 °C in a vacuum.

2.5 Adsorption of Congo Red

Adsorption experiments were conducted to evaluate dye adsorption of compound hydrogels. A series of conical flasks containing 10 mL Congo Red solution and 20.0 mg dry hydrogels were shaken at room temperature for a certain time. The initial and final concentration was analyzed by a UV-1780 spectrophotometer (Shimadzu, Japan) at 500 nm. Experiments were conducted at several times until the deviation was <1%. The adsorption capacity (q_e, mg g^{-1}) was defined using the following equation:

$$q_\mathrm{e} = \frac{C_0 - C_\mathrm{e}}{m} V \quad (2)$$

where C_0 and C_e are the initial and final concentrations of Congo Red solution, V is the volume of the dye solution, and m is the dry weight of adsorbents.

2.6 Equilibrium adsorption and rate constant studies

The equilibrium adsorption isotherm has an important role in the design of an adsorption system, and helps to describe the interactive behavior between adsorbents and solutes. The Freundlich equation is given as:

$$q_\mathrm{e} = K_\mathrm{F} {C_\mathrm{e}}^{1/n} \quad (3)$$

where K_F is the Freundlich constant (an indicator of the adsorption capacity (mg g^{-1})), C_e is the concentration of Congo Red after the adsorption equilibrium has reached (mg L^{-1}), and the magnitude of the exponent $1/n$ indicates adsorption ability. The value of n is >1, which represents a favorable adsorption condition.[22]

The widely used Langmuir isotherm is expressed as:

$$q_\mathrm{e} = \frac{q_\mathrm{m} K_\mathrm{L} C_\mathrm{e}}{K_\mathrm{L} C_\mathrm{e} + 1} \quad (4)$$

where q_m (g kg^{-1}) is the maximum adsorption under ideal conditions, C_e is the aqueous-phase sorbate concentration at equilibrium (mg L^{-1}), and K_L is the Langmuir isotherm constant (m^3 g^{-1}).

The pseudo-first order model (PFO), pseudo-second order model (PSO), and intraparticle diffusion model were employed to investigate the mechanism of adsorption. The formulae are shown as follows:

$$q_t = q_e(1 - e^{-k_1 t}) \quad (5)$$

$$q_t = \frac{k_2 q_e{}^2 t}{1 + t k_2 q_e} \quad (6)$$

$$q_t = k_{int} t^{0.5} + C_i \quad (7)$$

where q_t (mg g^{-1}) is the sorption amount at time t, q_e is the saturated adsorption amount, k_1, k_2 and k_{int} (g mg^{-1} min^{-1}) are the rate constant of the PFO, PSO and intraparticle diffusion models, respectively. As shown in formula (7), the higher value of C_i implies a greater boundary layer effect.

3. Results and discussion

3.1 Hydrogel formation and its images

Transparency is an effective way to detect if a polymer has blended well. The composite hydrogels were transparent and the background could be seen clearly even though the transparency was reduced with the addition of 5% REC (Scheme 1). The crosslinking reaction between chitosan and cellulose is caused by the nucleophilic reaction of ECH.[23]

Chemical crosslinking composite hydrogels could be easily formed with the required shape owing to the facile fabrication method and gel-forming ability. Hydrogels could be fabricated into different shapes by molds, which suggests that the composite hydrogels had good formability. Fig. 1a and b show that the composite hydrogels could be easily knotted and twisted without fracture due to their excellent flexibility. Also, Fig. 1c shows that the composite hydrogels could restore after compression, which implies that such hydrogels possess considerable resilience and high intensity. Fig. 1d is a photograph of the adsorption process of hydrogels. After a period of adsorption, the red solutions containing Congo Red become clear and transparent again, whereas the hydrogels turned red owing to the adsorption of dye. These images indicate that the composite hydrogels possess high toughness high intensity, and highly efficient dye adsorption.

3.2 Mechanical properties

Fig. 2 and Table 1 illustrate that all the hydrogels had excellent compressive intensity of >1 MPa. The strength of hydrogels was broadly proportional to the ratio of cellulose. A higher content of cellulose implied better mechanical properties. Hydrogels with a 1 : 9 mass ratio of chitosan : cellulose contained 90.0% water and obtained the maximum compressive strain (≤5.65 MPa). Thus, we could conclude that cellulose contributed to mechanical intensity and aimed to support the whole hydrogel, whereas chitosan had an important role in maintaining water and adsorbing the dye. Also, the compressive properties of hydrogels with different ratios of REC are shown in Fig. 2b. The hydrogels with 0%, 5% and 10% content of REC had a compressive strain of 1.48, 1.52 and 1.78 MPa, respectively. The compressive intensity of hydrogels increased with increasing amounts of REC. REC has good mechanical properties and a homogeneous distribution in alkali solutions.[24] Therefore, we could infer that REC could increase the mechanical behavior of composite hydrogels.

3.3 The surface structure of hydrogels

Fig. 3 shows the scanning electron microscopy (SEM) images of the composite hydrogels with the scale bar of 1 μm. It was

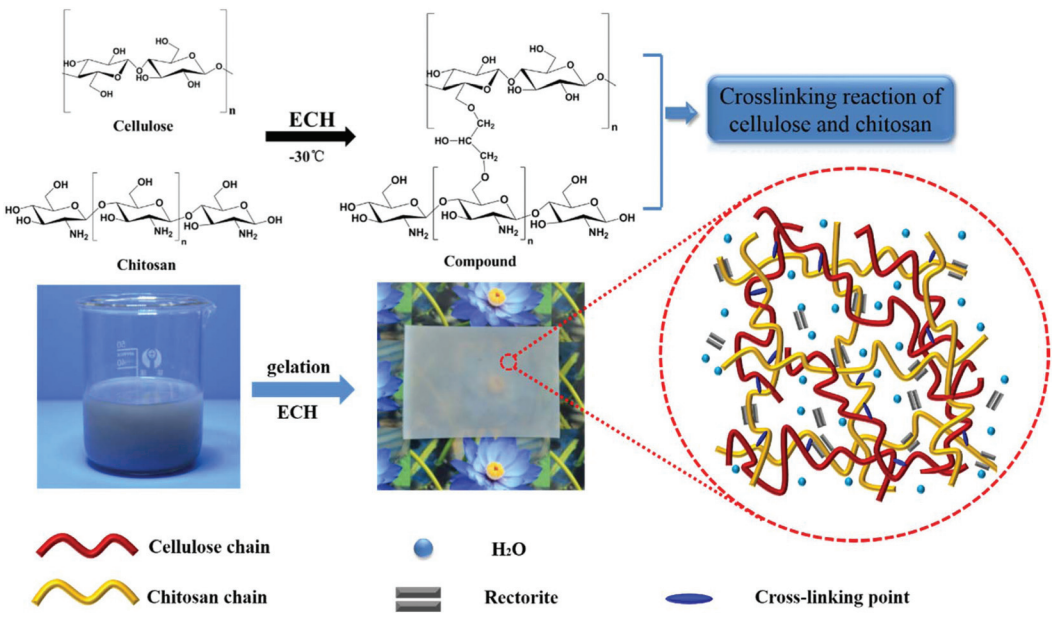

Scheme 1 Preparation of chitosan/REC/cellulose hydrogels by chemical crosslinking.

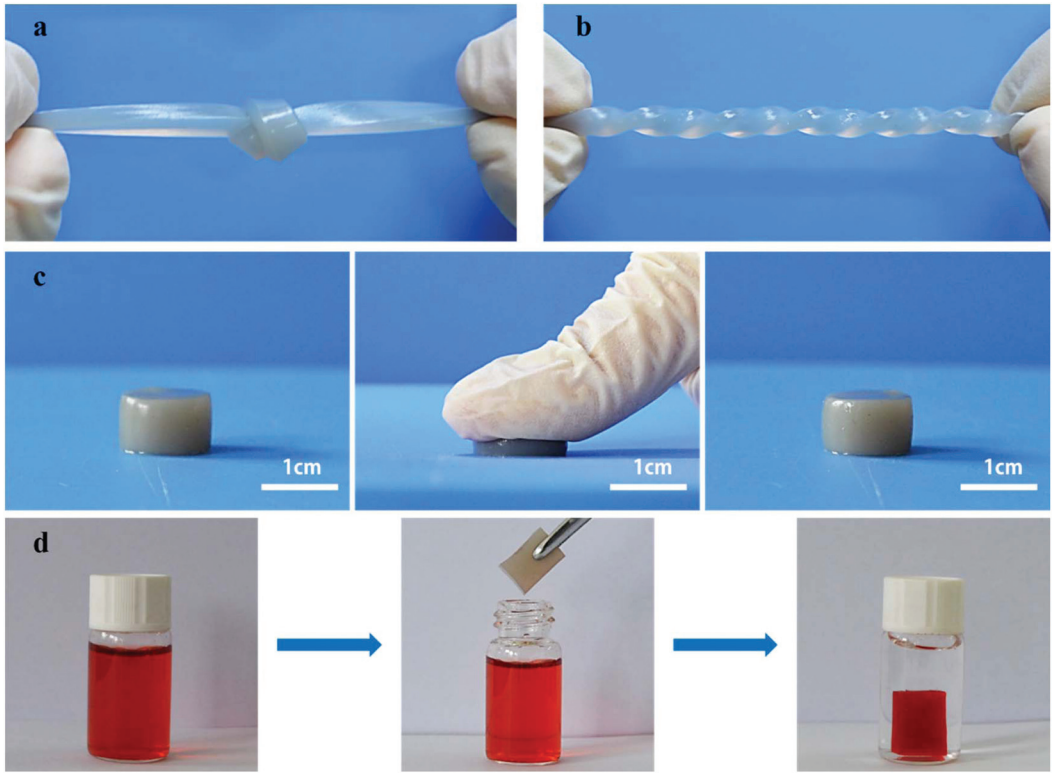

Fig. 1 Images of hydrogels with chitosan contents: cellulose = 3 : 1, 5% REC under (a) knotting, (b) twisting and (c) compression; (d) images of the adsorption of hydrogels (20 mg dry hydrogels were immersed in 15 mL Congo Red solutions at 100 mg L^{-1} for 2 h).

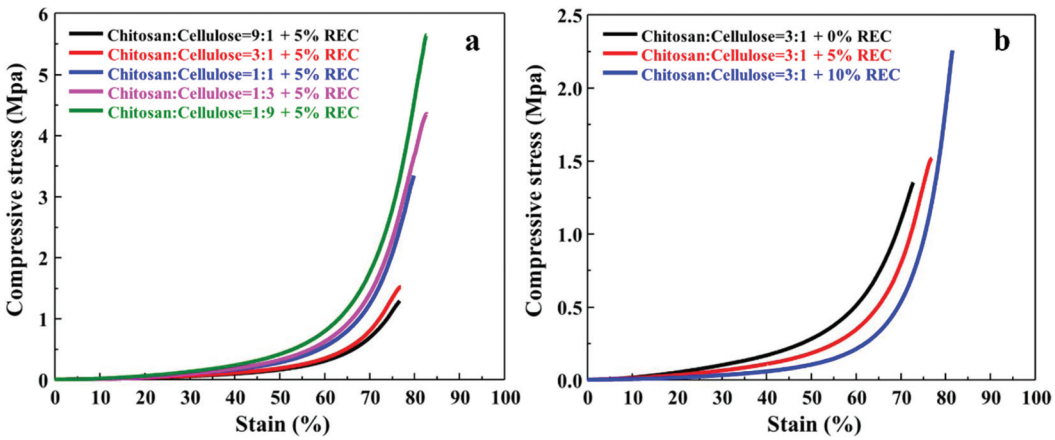

Fig. 2 Compressive properties of hydrogels with (a) a different mass ratio of chitosan/cellulose and (b) different proportions of REC.

obvious that all the hydrogels with different ratios of chitosan and cellulose had the interconnected, well-defined and three-dimensional porous structures that are beneficial for dye adsorption. When the content of REC was constant, with an increasing amount of chitosan, the composite hydrogels had larger apertures and contained more water, which could result in lower intensity and a higher swelling ratio. Comparison of Fig. 3b with Fig. 3c revealed that a larger amount of REC could reduce the possibility of the collapse of holes on the surface of hydrogels, which made the apertures of hydrogels well proportioned. The dense structure of hydrogels containing REC further contributed to improve the mechanical performance of hydrogels.[25] In addition, the energy-dispersive X-ray spectrum shown in Fig. 3f shows the characteristic peaks of Si and Al, which indicated that REC was introduced into chitosan/cellulose hydrogels.[15,26]

3.4 Composition analyses

The composition of hydrogels was analyzed with FT-IR and XPS. In the IR spectrum of chitosan, the adsorption band at

Table 1 The physical parameters of different types of hydrogels

Sample	Water content (%)	Compressive properties		
		σ (MPa)	ε (%)	E (MPa)
Chitosan : cellulose = 9 : 1 REC 5%	94.3	1.35	79.43	6.49
Chitosan : cellulose = 3 : 1 REC 5%	93.4	1.52	78.32	7.62
Chitosan : cellulose = 1 : 1 REC 5%	91.3	3.35	81.70	17.94
Chitosan : cellulose = 1 : 3 REC 5%	90.1	4.35	84.13	23.00
Chitosan : cellulose = 1 : 9 REC 5%	90.0	5.65	83.85	28.93
Chitosan : cellulose = 3 : 1 REC 0%	93.2	1.48	76.40	5.88
Chitosan : cellulose = 3 : 1 REC 10%	95.1	1.78	81.19	11.11

1655 cm^{-1} was caused by a C=O stretching vibration, whereas the band at 1590 cm^{-1} was assigned to the bending mode of –N–C=O.[27] As shown in FT-IR spectra, the peaks of composite hydrogels from 3300 to 3450 cm^{-1} corresponded to the stretching vibration of hydroxyl groups, which are the characteristic peaks of chitosan and cellulose.[15,28] Hence, the composites conserved the active groups of chitosan and cellulose for dye absorption during the formation process under an alkali/urea condition. However, the peaks of all the hydrogels at 1590 cm^{-1} had weak intensity because of the hydrogen bond formed among these ingredients.[29–31] In brief, the chemical structure of composite hydrogels became steadier through crosslinking. Furthermore, the peak at 545 cm^{-1} that represented the bending vibration of Si–O is a characteristic peak of REC.[32] It could be seen that the compound hydrogels also had a characteristic peak of Si–O, which is evidence of REC addition.

XPS revealed a wide-scan spectra of chitosan/cellulose hydrogels without or with a 5% weight ratio of REC. Both samples had almost the same proportion of C, O and N. Also, chitosan/REC/cellulose hydrogels showed the binding energy of Si2p, which was identical with the results of EDS.

3.5 Swelling behavior

Fig. 4 displays the swelling behavior of hydrogels under different pH conditions. Due to the addition of ECH, the hydrogels could not be dissolved even under acid conditions.[33] The hydrogels exhibited clear pH-responsive swelling behavior, which was significant at low pH. Also, the swelling ability declined when the content of cellulose increased. Hydrogels with a 9 : 1 weight ratio of chitosan : cellulose had the largest swelling ratio (72%) at a pH of 2, whereas hydrogels with 1 : 9 weight ratio of chitosan : cellulose had the smallest swelling ratio (8%). A reasonable explanation is that the capability of water adsorption was relative to the crosslinking degree of hydrogels.[34] With an increasing amount of cellulose, hydrogen bonds could be formed between polymers and the crosslinking agent. Such hydrogen bonds eventually formed a steadier structure that prevented traversing of water molecules which, ultimately, led to lower swelling ratio.[35] In addition, when hydrogels were under an acid condition, the $-NH_2$ in chitosan would attract the H^+ in water and became $-NH_3$. The electrostatic force became unbalanced, resulting in stronger electrostatic repulsion, which finally led to the expansion of the hydrogel networks.[36]

3.6 Specific surface area and pore-size analyses

The BET adsorption isotherms of composite hydrogels were also measured. All the adsorption/desorption isotherms had closed loop circuits without superposition, which were caused by the hysteresis effect.[37] The isotherms of samples were steep; that is, composite hydrogels possessed a distinguishable cylindrical pore structure with open ends.[38] Also, the surface area of hydrogels with a 9 : 1 weight ratio of chitosan : cellulose displayed the largest surface area among all the samples

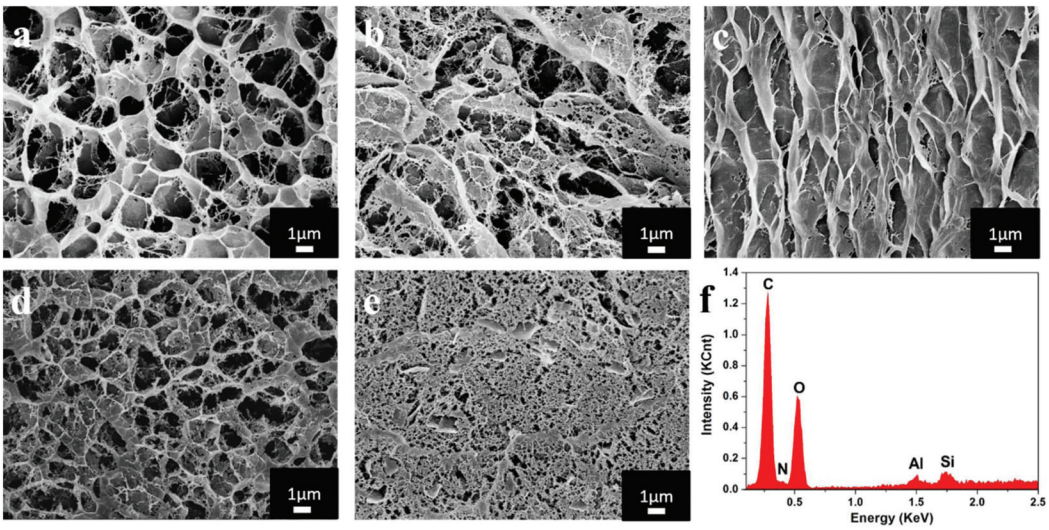

Fig. 3 SEM images of hydrogels with a weight ratio of (a) chitosan : cellulose = 9 : 1, 5% REC; (b) chitosan : cellulose = 3 : 1, 5% REC; (c) chitosan : cellulose = 3 : 1, 10% REC; (d) chitosan : cellulose = 1 : 1, 5% REC; (e) chitosan : cellulose = 1 : 9, 5% REC and (f) EDS spectrum of sample b.

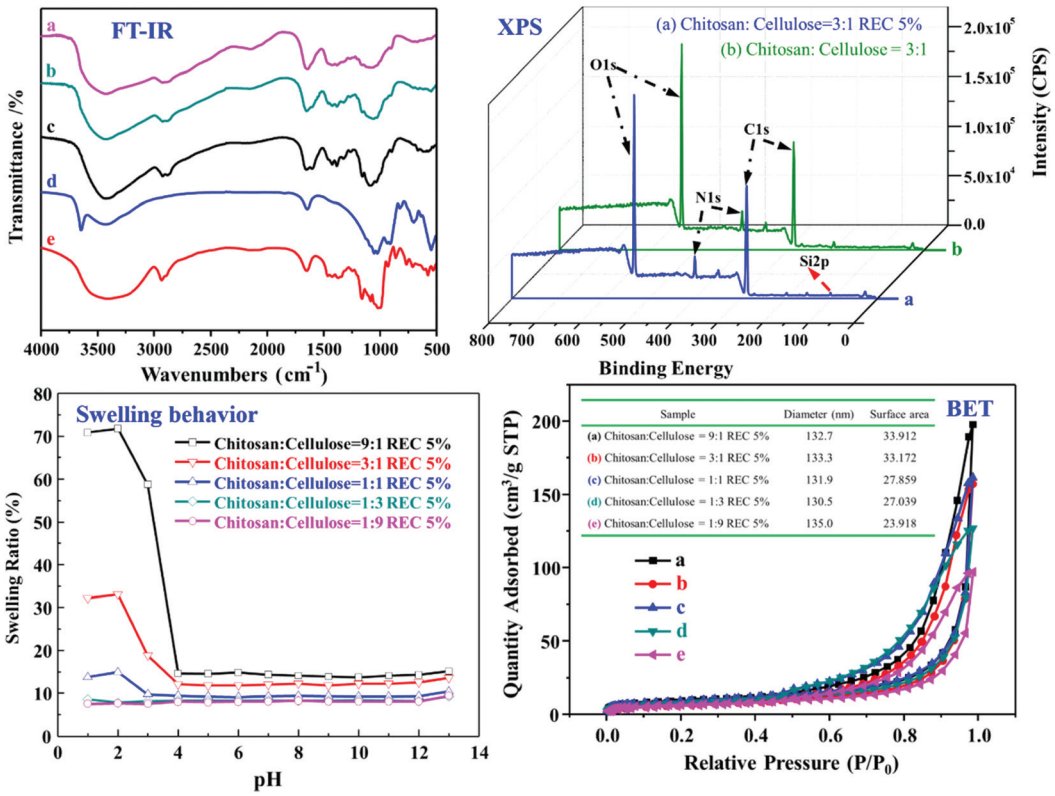

Fig. 4 The FT-IR spectra of hydrogels with a weight ratio of (a) chitosan : cellulose = 1 : 3, 5% REC, (b) chitosan : cellulose = 3 : 1, 5% REC, (c) chitosan, (d) REC and (e) cellulose; the XPS spectra of different types of hydrogels; the swelling behaviors of various hydrogels under different pH conditions; BET adsorption isotherms of compound hydrogels.

tested. In addition, the surface area of the composite hydrogels decreased with an increasing weight ratio of cellulose, similar to the SEM results.

3.7 XRD patterns

XRD was performed to examine the crystallinity of various hydrogels. Chitosan had characteristic diffraction peaks at 2θ = 10.7° and 20.0°,[39] whereas the peaks for cellulose I were at 2θ = 15.1° and 22.6° (Fig. 5).[40] Also, the compound hydrogels had an X-ray diffraction peak at 2θ = 20.03°, which showed a slight shift compared with the raw ingredients. This phenomenon indicated that the crystal structure of cellulose changed from type I to type II due to chemical crosslinking with chitosan.[23] The compact arrangement of hydrogen bonds in cellulose II could improve the physical properties of the compound hydrogels, such as thermostability and mechanical strength. In addition, the characteristic diffraction peaks of REC are at 2θ = 7.96° and 20.05°,[41] which could be also seen in the patterns of composite hydrogels. Contrasting the sharpness and half-peak width of all composite hydrogels suggested that hydrogels with a greater content of REC had better crystallinity.[42]

3.8 Thermostability testing

Chitosan/cellulose hydrogels had lower degradative temperature but a higher amount of residue than chitosan and cellulose (Fig. 5). This was probably caused by the change of crystallinity and structure after crosslinking.[43] Also, chitosan/REC/cellulose hydrogels had higher mass residue compared with pure chitosan and cellulose because REC, as an inorganic material, had little mass loss when heated ≤600 °C. In addition, the initial degradation temperature and T_{max} of hydrogels increased after REC addition, so thermal stability was enhanced.

3.9 Adsorption of Congo Red

The effect of adsorbents with different mass ratios on adsorption property is shown in Table 2. Here, the initial concentration of Congo Red was 100 mg L^{-1} and the initial volume was 25 mL. It was obvious that the saturated adsorption capacity increased when the content of chitosan was higher. Additionally, when the ratio of chitosan : cellulose was constant (3 : 1), the saturated adsorption capacity of composite hydrogels increased with an increasing amount of REC. This phenomenon could have been because the exchangeable hydrated cations in REC had been exchanged with the dye cations.[20,44] Hence, we could conclude that chitosan was the main functional material for adsorption, REC assisted adsorption, and cellulose supported the structure. After taking the factors of cost, adsorption effects and intensity into consideration, we chose hydrogels with a 3 : 1 weight ratio of chitosan : cellulose and 5% REC for subsequent experiments.

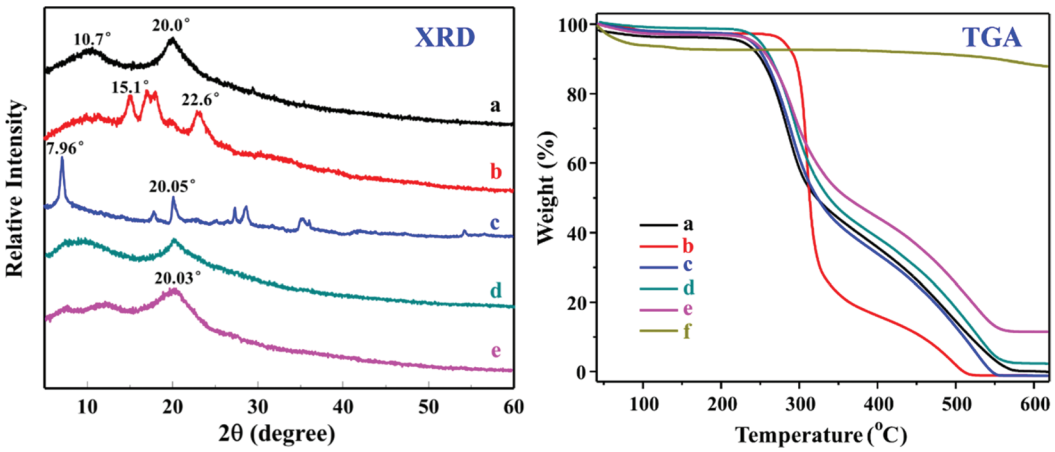

Fig. 5 XRD patterns of powder and compound hydrogels: (a) chitosan, (b) cellulose, (c) REC, (d) chitosan : cellulose = 3 : 1, 5% REC and (e) chitosan : cellulose = 1 : 3, 5% REC; TGA thermograms of samples: (a) chitosan, (b) cellulose, (c) chitosan : cellulose = 3 : 1, 0% REC, (d) chitosan : cellulose = 3 : 1, 5% REC, (e) chitosan : cellulose = 3 : 1, 10% REC and (f) REC.

Table 2 The saturated adsorption capacity of different sorbents

Sample	q_e (mg g^{-1})
Chitosan : cellulose = 9 : 1 REC 5%	57.44
Chitosan : cellulose = 3 : 1 REC 5%	47.32
Chitosan : cellulose = 1 : 1 REC 5%	38.70
Chitosan : cellulose = 1 : 3 REC 5%	35.98
Chitosan : cellulose = 1 : 9 REC 5%	34.36
Chitosan : cellulose = 3 : 1 REC 0%	46.53
Chitosan : cellulose = 3 : 1 REC 10%	51.53

Fig. 6a and b show the influence on saturated adsorption capacity by the initial concentration of Congo Red and reaction time, respectively. In Fig. 6a, the saturated adsorption capacity of compound hydrogels increased with an increasing initial concentration of Congo Red. When the initial concentration of Congo Red was 10, 100 and 500 mg L^{-1}, the saturated adsorption amount of hydrogels was 4.47, 48.13 and 166.10 mg g^{-1}, respectively. The removal rate was ≈100% when the initial concentration was <100 mg L^{-1} yet, if the initial concentration increased further, the removal rate declined. A reasonable explanation for this finding was that the amount of Congo Red with a lower initial concentration was small, which made adsorption easy. When the initial concentration continued to increase, the surface of sorbents had no more functional sites for adsorption.

The adsorption rate increased extremely rapidly at the beginning, then gradually slowed down and, finally, reached an equilibrium (Fig. 6b). This phenomenon happened because the composite hydrogels had many free functional sites initially, and would react with the Congo Red molecules as soon as they came into contact. However, the increasing numbers of molecules combining on the surface of sorbents would repel free Congo Red molecules over time, resulting in a lower adsorption rate. When repellant and driving forces reached a balance, the reaction equilibrium would be reached, and adsorption would not be influenced by the reaction time any more. Wang *et al.* prepared chitosan/montmorillonite nanocomposites for Congo Red adsorption, and the amount of

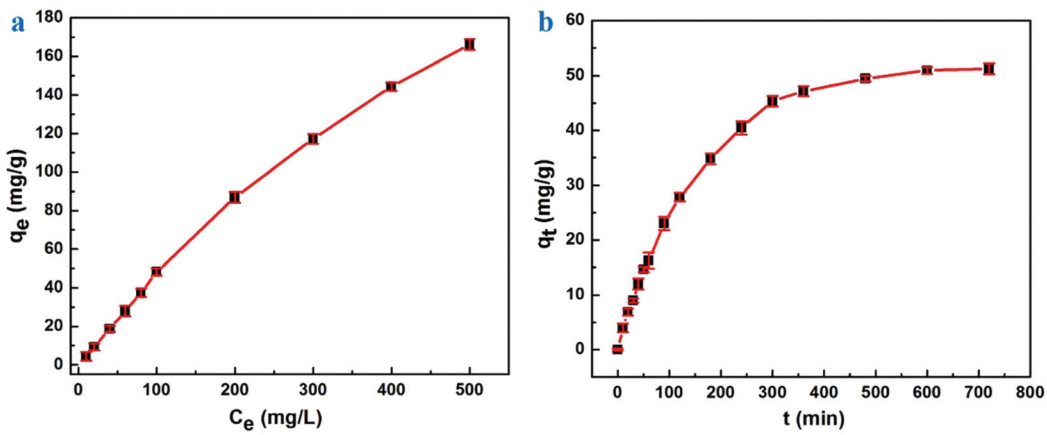

Fig. 6 Saturated adsorption capacity: (a) under an different initial concentration of Congo Red, (b) at different reaction times.

saturated adsorption was <100 mg g^{-1},[45] which was much lower than that of our hydrogels. Woo *et al.* have undertaken several studies on chitosan materials for dye adsorption.[46,47] They fabricated chitosan-based hydrogel beads that possessed an adsorption amount of 380 mg g^{-1}. Although our materials showed weaker adsorption capacity, our hydrogels had stronger mechanical properties and higher adsorption rate. At present, some materials have a larger saturated adsorption amount to various dyes than our hydrogels. Hence, a considerable amount of work must be done to increase the adsorption amount of our materials in future studies.

3.10 Adsorption mechanisms and kinetics

The adsorption mechanisms were investigated by Freundlich and Langmuir isotherm models (Fig. 7). The Freundlich adsorption isotherm had a correlation coefficient (R^2) of 0.994 and the exponent (n) was 10.78, hence, the sorption data closely fitted with the Freundlich model. However, the low R^2 (0.9034) revealed poor agreement with the Langmuir isotherm according to experimental data. In summary, these models demonstrated that the composite hydrogels exhibited excellent adsorption capacity, and the adsorption was in accordance with the Freundlich model.

Kinetics models were also applied to identify the rate of adsorption. The PSO kinetic model showed better agreement of experimental data (R^2 > 0.99) than the PFO kinetic model and intra-particle diffusion model (Fig. 7). These results suggested that the main adsorption mechanism was chemical adsorption involving the sharing and transfer of electrons, and did not involve the mass transfer of solution.[48] The adsorption rate was determined by the free adsorption site on the surface of the adsorbent.

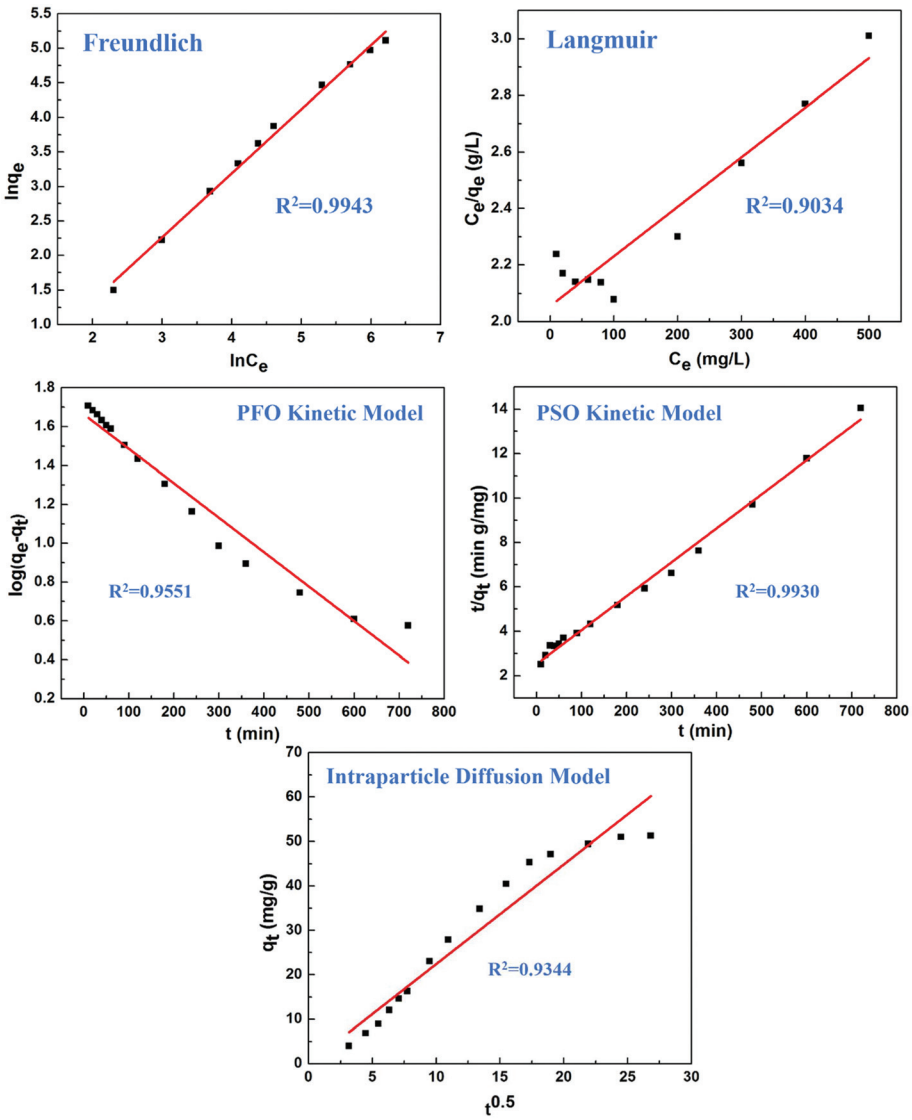

Fig. 7 The adsorption isotherm and adsorption kinetic equations for explaining adsorption mechanisms.

4. Conclusion

We succeeded in constructing chitosan/rectorite/cellulose hydrogels using environmental friendly materials with a green method. The prepared hydrogels were convenient to be utilized, easy to access, low cost, and exhibited high strength and elasticity. Also, the hydrogels had outstanding adsorption ability towards dye in wastewater. In addition, the incorporation of REC was conducive to further increase the saturated adsorption capacity. Hydrogels with higher strength may be more competitive than general products for industrial application. Additionally, the hydrogels used here could be employed for the other applications, such as heavy-metal adsorption.

Acknowledgements

This work was supported by the National Natural Science Foundation of China (grant number 51473125) and partially supported by the Natural Science Foundation of Hubei Province of China (Team Project, number 2015CFA017).

References

1 K. Tanaka, K. Padermpole and T. Hisanaga, *Water Res.*, 2000, **34**, 327–333.
2 T. Robinson, G. Mcmullan, R. Marchant and P. Nigam, *Bioresour. Technol.*, 2001, **77**, 247.
3 W. S. W. Ngah, L. C. Teong and M. A. K. M. Hanafiah, *Carbohydr. Polym.*, 2011, **83**, 1446–1456.
4 L. Li, W. Smitthipong and H. Zeng, *Polym. Chem.*, 2014, **6**, 353–358.
5 X. Luo, J. Zeng, S. Liu and L. Zhang, *Bioresour. Technol.*, 2015, **194**, 403–406.
6 S. B. Yu, L. Hao, J. Tian, H. Wang, D. W. Zhang, Y. Liu and Z. T. Li, *Polym. Chem.*, 2016, **7**, 3392–3397.
7 A. Gandini, *Polym. Chem.*, 2009, **1**, 245–251.
8 Y. Yang, S. Wang, Y. Wang, X. Wang, Q. Wang and M. Chen, *Biotechnol. Adv.*, 2014, **32**, 1301–1316.
9 J. N. Tiwari, K. Mahesh, N. H. Le, K. C. Kemp, R. Timilsina, R. N. Tiwari and K. S. Kim, *Carbon*, 2013, **56**, 173–182.
10 Q. Wang, H. Cheng, H. Peng, H. Zhou, P. Y. Li and R. Langer, *Adv. Drug Delivery Rev.*, 2014, **91**, 125.
11 X. Hu, Y. Tang, Q. Wang, Y. Li, J. Yang, Y. Du and J. F. Kennedy, *Carbohydr. Polym.*, 2011, **83**, 1128–1133.
12 C. K. S. Pillai, W. Paul and C. P. Sharma, *Prog. Polym. Sci.*, 2009, **34**, 641–678.
13 Q. Wang, Z. Gu, S. Jamal, M. S. Detamore and C. Berkland, *Tissue Eng.*, 2013, **19**, 2586–2593.
14 J. Tian, H. Tu, X. Shi, X. Wang, H. Deng, B. Li and Y. Du, *Colloids Surf., B*, 2016, **145**, 643.
15 H. Tu, Y. Lu, Y. Wu, J. Tian, Y. Zhan, Z. Zeng, H. Deng and L. Jiang, *Int. J. Pharm.*, 2015, **493**, 426–433.
16 Q. Wang, *Smart Materials for Tissue Engineering: Fundamental Principles*, Royal Society of Chemistry, 2016.
17 R. Roeder, O. Garcíavaldez, R. Whitney, P. Champagne and M. F. Cunningham, *Polym. Chem.*, 2016, 6383–6390.
18 M. H. Beyki, M. Bayat and F. Shemirani, *Bioresour. Technol.*, 2016, **218**, 326–334.
19 W. L. Ijdo, T. Lee and T. J. Pinnavaia, *Adv. Mater.*, 1996, **8**, 79–83.
20 D. Wu, P. Zheng, P. R. Chang and X. Ma, *Chem. Eng. J.*, 2011, **174**, 489–494.
21 Y. Lu, P. R. Chang, P. Zheng and X. Ma, *Chem. Eng. J.*, 2014, **255**, 49–54.
22 M. S. Chiou and H. Y. Li, *J. Hazard. Mater.*, 2002, **93**, 233–248.
23 D. Zhao, J. Huang, Y. Zhong, K. Li, L. Zhang and J. Cai, *Adv. Funct. Mater.*, 2016, **26**, 6279–6287.
24 C. Belver and M. A. Vicente, *Chem. Mater.*, 2002, **14**, 2033–2043.
25 J. Fan, Z. Shi, M. Lian, H. Li and J. Yin, *J. Mater. Chem. A*, 2013, **1**, 7433–7443.
26 S. Xin, Z. Zeng, X. Zhou, W. Luo, X. Shi, Q. Wang, H. Deng and Y. Du, *J. Hazard. Mater.*, 2017, **324**, 365–372.
27 A. Sionkowska, M. Wisniewski, J. Skopinska, C. J. Kennedy and T. J. Wess, *Biomaterials*, 2004, **25**, 795–801.
28 S. A. Paralikar, J. Simonsen and J. Lombardi, *J. Membr. Sci.*, 2008, **320**, 248–258.
29 S. Wang, A. Lu and L. Zhang, *Prog. Polym. Sci.*, 2015, **53**, 169–206.
30 F. Ding, H. Deng, Y. Du, X. Shi and Q. Wang, *Nanoscale*, 2014, **6**, 9477–9493.
31 X. Li, Y. Han, Y. Ling, X. Wang and R. Sun, *ACS Sustainable Chem. Eng.*, 2015, **3**, 1846–1852.
32 F. Kooli, J. Bovey and W. Jones, *J. Mater. Chem.*, 1997, **7**, 153–158.
33 C. Y. Chen, J. C. Chang and A. H. Chen, *J. Hazard. Mater.*, 2011, **185**, 430–441.
34 K. Haraguchi and T. Takehisa, *Adv. Mater.*, 2002, **14**, 1120–1124.
35 J. Cai, S. Liu, J. Feng, S. Kimura, M. Wada, S. Kuga and L. Zhang, *Angew. Chem., Int. Ed.*, 2012, **51**, 2076–2079.
36 J. Duan, X. Liang, Y. Cao, S. Wang and L. Zhang, *Macromolecules*, 2015, **48**, 2706–2714.
37 T. Cheng, R. He, Q. Zhang, X. Zhan and F. Chen, *J. Mater. Chem. A*, 2015, **3**, 21637–21646.
38 L. Heath and W. Thielemans, *Green Chem.*, 2010, **12**, 1448–1453.
39 Z. G. Chen and P. Wang, *Acta Biomater.*, 2009, **6**, 372–382.
40 A. D. French and G. P. Johnson, *Cellulose*, 2004, **11**, 5–22.
41 G. Zhang, Y. Gao, Y. Zhang and Y. Guo, *Environ. Sci. Technol.*, 2010, **44**, 6384–6389.
42 C. Guan, C. Lü, Y. Cheng, S. Song and B. Yang, *J. Mater. Chem.*, 2008, **19**, 4062–4068.
43 S. C. M. Fernandes, B. L. U. Oliveira, A. C. S. R. Freire and A. A. J. D. Silvestre, *Green Chem.*, 2009, **11**, 2023–2029.
44 Y. Zheng and A. Wang, *J. Hazard. Mater.*, 2009, **171**, 671–677.
45 L. Wang and A. Wang, *J. Hazard. Mater.*, 2007, **147**, 979.
46 S. Chatterjee, M. W. Lee and S. H. Woo, *Bioresour. Technol.*, 2010, **101**, 1800–1806.
47 S. Chatterjee, *Bioresour. Technol.*, 2009, **100**, 3862–3868.
48 W. H. Cheung, Y. S. Szeto and G. Mckay, *Bioresour. Technol.*, 2007, **98**, 2897–2904.